An experimentally supported model for the origin of charge transport barrier in Zn(O,S)/CIGSSe solar cells

Chua, Rou Hua; Li, Xianglin; Walter, Thomas; Teh, Lay Kuan; Hahn, Thomas; Hergert, Frank; Mhaisalkar, Subodh; Wong, Lydia Helena

2016

Chua, R. H., Li, X., Walter, T., Teh, L. K., Hahn, T., Hergert, F., Mhaisalkar, S., et al. (2016). An experimentally supported model for the origin of charge transport barrier in Zn(O,S)/CIGSSe solar cells. Applied Physics Letters, 108(4), 043505-.

https://hdl.handle.net/10356/82433

https://doi.org/10.1063/1.4940913

AIP | Applied Physics Letters

An experimentally supported model for the origin of charge transport barrier in Zn(O,S)/CIGSSe solar cells

Rou Hua Chua, Xianglin Li, Thomas Walter, Lay Kuan Teh, Thomas Hahn, Frank Hergert, Subodh Mhaisalkar, and Lydia Helena Wong

Citation: Applied Physics Letters **108**, 043505 (2016); doi: 10.1063/1.4940913
View online: http://dx.doi.org/10.1063/1.4940913
View Table of Contents: http://scitation.aip.org/content/aip/journal/apl/108/4?ver=pdfcov
Published by the AIP Publishing

An experimentally supported model for the origin of charge transport barrier in Zn(O,S)/CIGSSe solar cells

Rou Hua Chua,[1,2,3] Xianglin Li,[1] Thomas Walter,[4] Lay Kuan Teh,[3] Thomas Hahn,[5] Frank Hergert,[5] Subodh Mhaisalkar,[1,2] and Lydia Helena Wong[1,2,a)]
[1]*Energy Research Institute @ NTU (ERI@N), Interdisciplinary Graduate School, Nanyang Technological University, Singapore 639798*
[2]*School of Materials Science and Engineering, Nanyang Technological University, Singapore 639798*
[3]*Robert Bosch (SEA) Pte Ltd, 11 Bishan St. 21, Singapore 573943*
[4]*Hochschule Ulm, Albert-Einstein-Allee 55, 89081 Ulm, Germany*
[5]*Bosch Solar CISTech GmbH, Münstersche Str. 24, 14772 Brandenburg an der Havel, Germany*

(Received 10 September 2015; accepted 15 January 2016; published online 27 January 2016)

Zinc oxysulfide buffer layers with [O]:[S] of 1:0, 6:1, 4:1, 2:1, and 1:1 ratios were deposited by atomic layer deposition on $Cu(In,Ga)(S,Se)_2$ absorbers and made into finished solar cells. We demonstrate using Time-Resolved Photoluminescence that the minority carrier lifetime of Zn(O,S) buffered solar cells is dependent on the sulfur content of the buffer layer. τ_1 for devices with [O]:[S] of 1:0–4:1 are <10 ns, indicating efficient charge separation in devices with low sulfur content. An additional τ_2 is observed for relaxed devices with [O]:[S] of 2:1 and both relaxed and light soaked devices with [O]:[S] of 1:1. Corroborated with one-dimensional electronic band structure simulation results, we attribute this additional decay lifetime to radiative recombination in the absorber due to excessive acceptor-type defects in sulfur-rich Zn(O,S) buffer layer that causes a buildup in interface-barrier for charge transport. A light soaking step shortens the carrier lifetime for the moderately sulfur-rich 2:1 device when excess acceptors are passivated in the buffer, reducing the crossover in the dark and illuminated I-V curves. However, when a high concentration of excess acceptors exist in the buffer and cannot be passivated by light soaking, as with the sulfur-rich 1:1 device, then cell efficiency of the device will remain low. © *2016 AIP Publishing LLC*. [http://dx.doi.org/10.1063/1.4940913]

Zinc oxysulfide (Zn(O,S), $E_g = 3.0$–3.6 eV) is increasingly replacing cadmium sulfide (CdS, $E_g = 2.4$ eV) as a buffer layer for $Cu(In,Ga)(S,Se)_2$ (CIGSSe) devices, due to environmental concerns with cadmium and potential for higher current density for wider bandgap Zn(O,S).[1] A metastable solar cell experiences a drop in cell efficiency during dark storage as shown by (1) a crossover of the dark and illuminated I-V curves and (2) fill factor (*FF*) loss accompanied by a kink in the illuminated I-V curve.[2–4] Although charge transport issues arise with Zn(O,S) buffered devices during prolonged dark storage,[3,5] this can be mitigated by a light soaking step. This efficiency loss has been suggested to originate from the [O]:[S] ratio of Zn(O,S) which alters the buffer bandgap[6] and conduction band offset (CBO) between the Zn(O,S)/CIGSSe interface.[7] On one hand, sulfur-poor Zn(O,S) tends to form oxygen (V_O) or sulfur vacancies (V_S), which are donor states, whereas a sulfur-rich Zn(O,S) buffer tends to have a higher concentration of zinc vacancies (V_{Zn}) or sulfur interstitials (S_i), which leads to acceptor states in the bulk of the buffer layer.[8] This increase in acceptors has been modelled by the SCAPS-1D[9] simulation to influence the electric field strength of the p-n heterojunction. In this paper, we demonstrate that atomic layer deposition (ALD) Zn(O,S) buffered solar cells with increasing sulfur content showed increased metastability. This resulted from the reduction of charge separation strength and increasing recombination in sulfur-rich devices, as supported by an investigation on charge carrier recombination kinetics using Time Resolved Photoluminescence (TRPL). This experimental observation is validated with the SCAPS-1D simulation,[9] in order to explain a likely mechanism of metastability in the CIGSSe devices that is most apparent with sulfur-rich Zn(O,S).

The CIGSSe thin films were deposited on molybdenum coated glass substrates by a two-step sputtering process as described by Probst *et al.*[10] Zn(O,S) buffer was deposited by ALD on the CIGSSe absorbers cleaned with 2.5% NH_3(aq).[11] This was carried out in a Cambridge Nanotec Fiji 200 system using diethylzinc ($Zn(C_2H_5)_2$, DEZ, Aldrich, >99%), H_2O (18 MΩ cm), and H_2S (2.5% balanced in Ar) as the zinc, oxygen, and sulfur sources, respectively. The reaction chamber and the precursor delivery line were maintained at 120 °C throughout the experiments. During deposition, a 40 sccm high purity argon gas was used for the process and purging. Chamber pressure was maintained at 106 Pa. The DEZ:Ar:H_2O or H_2S:Ar pulse cycle had a pulse length of 0.08:10:0.08 s for H_2O or 0.1:10 s for H_2S. In order to vary the stoichiometric ratio of O and S with ALD in each device, the ratio of DEZ:Ar:H_2O:Ar to DEZ:Ar:H_2S:Ar was modified for each device. The number of pulses of DEZ:Ar:H_2O:Ar per DEZ:Ar:H_2S:Ar pulse per cycle directly corresponded to [O]:[S] = 1:0, 6:1, 4:1, 2:1, and 1:1, and the exact stoichiometries were verified afterwards with X-ray photoemission spectroscopy (XPS).

a)Author to whom correspondence should be addressed. Electronic mail: lydiawong@ntu.edu.sg.

The growth rates of ALD ZnO and ZnS at 120 °C were calibrated to be 0.18 nm/cycle and 0.13 nm/cycle as described by Woollam.[12] All buffers prepared on absorbers were ~50 nm thick. Devices with [O]:[S] = 1:0, 6:1, and 4:1 ratios are hereby labelled as sulfur-poor Zn(O,S) and those with [O]:[S] = 2:1 and 1:1 ratio, sulfur-rich Zn(O,S). The semi-finished layers were completed by the deposition of a transparent i-ZnO/ZnO:Al front contact and an Al/Ni contact grid. The full devices produced efficiencies ranging from 0% to 15% as-fabricated. Light soaking was performed for 4 h on relaxed devices with a Xenon lamp as sun simulator with 100 mW cm^{-2}.

In a typical TRPL experiment, a solar cell with the layer stack sequence of Mo/CIGSSe/Zn(O,S)/i-ZnO/ZnO:Al was excited with a 650 nm wavelength laser generated by a quartz laser system at room temperature. With a pulse rate of 5 MHz, and a beam diameter of 1 μm, the injection level was fixed at $I_o \sim 5 \times 10^7$ photons cm^{-2} per pulse. Since the penetration depth into the absorber was calculated to 0.2 μm, this results in a generation density of 3.16×10^7 photons cm^{-2} s^{-1} which is much lower than 1 Sun condition (~10^{17} photons cm^{-2} s^{-1}), hence I_o is defined to be low injection. With this condition, we can assume open circuit conditions with no photo-voltage buildup. The PL decay curves were measured in the approximate wavelength range of 1200–1300 nm by a Germanium avalanche photo-diode detector cooled with liquid N_2 with time-correlated single-photon counting.[13]

A VG ESCALAB 220i-XL system equipped with a concentric hemispherical energy analyzer was used for XPS to determine different Zn(O,S) compositions deposited on the absorber by ALD. The light source consists of a monochromatic Al Kα (1486.6 eV) for XPS characterization. A magnetic immersion lens was used to maximize the signal. Quantitative analysis was performed by first using a Shirley background subtraction before performing a least-square-error fit using a mixture of Gaussian-Lorentzian lineshapes.[14] Care was taken to ensure reasonable values for all the full width at half-maximum (FWHM) of the fitted components. The relative atomic concentrations were then calculated after taking into account the instrument transmission function together with the Scofield photoionization sensitivity factor.[15] All core-level peaks were references by assigning the adventitious carbon peak to 284.6 eV.

Electrical measurements were performed at room temperature using a Rotating Parallel Dipole Line AC Hall System.[16] The 100 nm thick quartz samples of 0.25 mm^2 were used to determine the electrical properties. Resistivity, carrier concentration, and electron mobility values were the average of three measurements.

I-V characterization was performed for devices after dark storage (i.e., relaxed state) which was subsequently light soaked under 1 Sun condition for 4 h and measured again. The corresponding dark/illumination curves are plotted in Figs. 1(a)–1(c) for sulfur-poor ([O]:[S] = 1:0–4:1), moderately sulfur-rich ([O]:[S] = 2:1) and highly sulfur rich ([O]:[S] = 1:1 Zn(O,S) devices, respectively. The moderately sulfur-rich 2:1 device had a crossover feature in its relaxed and light soaked state, suggesting metastability due to charge transport issue, which was not observed for the sulfur-poor devices. The highly sulfur-rich 1:1 device had distorted I-V features at both relaxed and light soaked state.

The TRPL spectra for sulfur-poor and sulfur-rich Zn(O,S) are plotted in Figs. 1(d)–1(f), respectively, to clearly distinguish the decay lifetime(s). The detected PL intensity

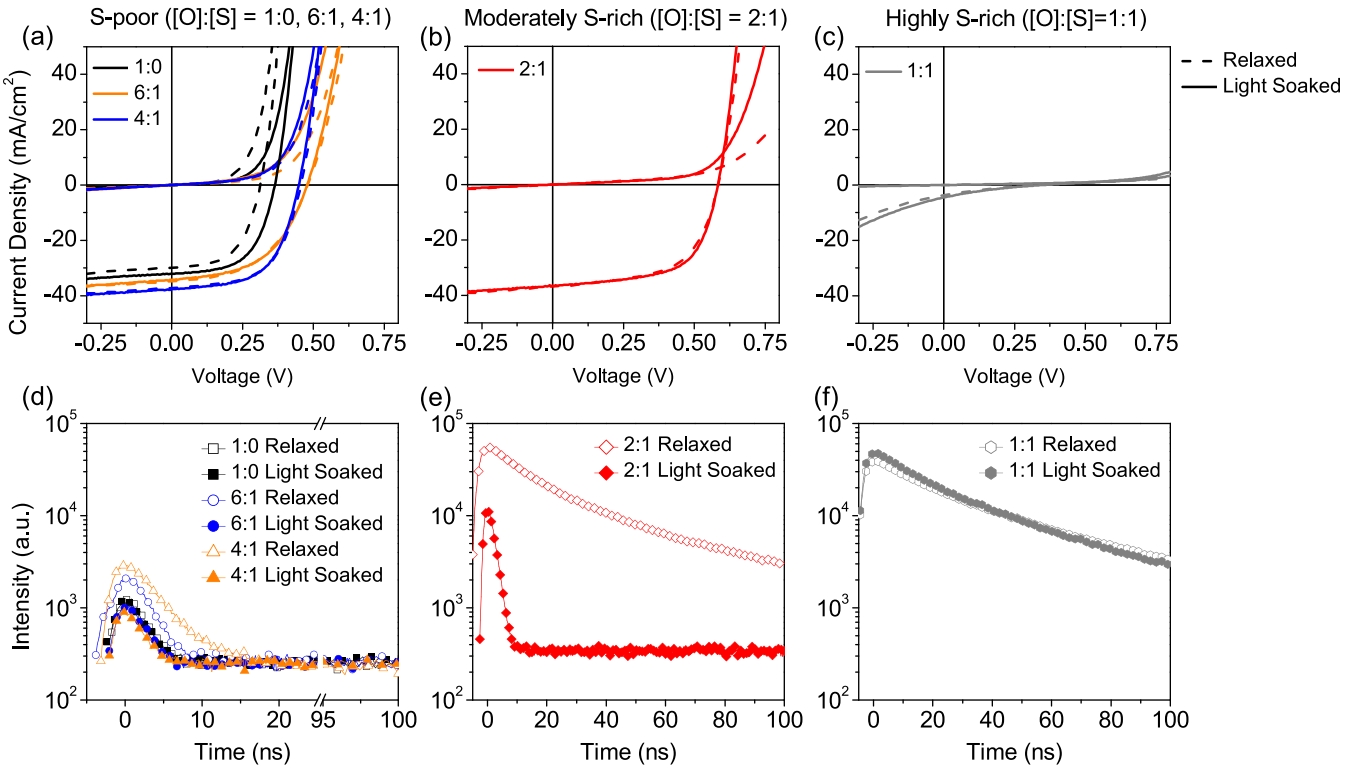

FIG. 1. I-V curves of relaxed (dashed lines) and light soaked (LS) (solid lines) Zn(O,S) buffered devices with (a) sulfur-poor ([O]:[S] = 1:0, 6:1, 4:1), (b) moderately sulfur-rich ([O]:[S] = 2:1) buffer, (c) highly sulfur-rich ([O]:[S] = 1:1) buffer and their respective lifetimes for (d) sulfur-poor, (e) moderately sulfur-rich, and (f) highly sulfur-rich devices determined by the single or bi-exponential decay fittings of the TRPL spectra, respectively.

TABLE I. Decay lifetimes of relaxed and light soaked (LS) devices with Zn(O,S) [O]:[S] = 1:0, 6:1, 4:1, 2:1, and 1:1 determined by the single or bi-exponential decay fitting of the TRPL spectra).

[O]:[S]	Condition	τ_1 (ns)	τ_2 (ns)	Intensity $\times 10^4$ (a.u.)	V_{OC} (V)	J_{SC} (mA/cm^2)	FF	Eff (%)
1:0	Relaxed	5.67	…	0.1	0.31	29.9	56	5.2
	LS	8.45	…	0.09	0.37	32.1	57	6.8
6:1	Relaxed	5.29	…	0.18	0.48	34.9	50	8.4
	LS	4.13	…	0.07	0.48	34.3	51	8.4
4:1	Relaxed	4.82	…	0.27	0.45	37.1	59	9.9
	LS	6.56	…	0.07	0.45	37.6	58	9.8
2:1	Relaxed	9.89	29.4	5.52	0.59	37.0	58	12.7
	LS	6.36	…	1.21	0.59	36.7	62	13.4
1:1	Relaxed	14.8	46.0	3.91	0.34	3.7	19	0.2
	LS	15.2	45.5	4.82	0.35	4.5	18	0.3

is tabulated in Table I. For the sulfur-poor devices and the light soaked moderately sulfur-rich device, we fit the exponential decay[17] after subtracting a constant background intensity to derive the sweep out time of carriers[18]

$$I_{PL}(t) = A_1 e^{\frac{-t}{\tau_1}}, \quad (1)$$

where t is time and A_1 is a fitting constant. For the rest of the relaxed and light soaked sulfur-rich devices, a bi-exponential decay was fitted to account for both τ_1 and a longer decay lifetime commonly associated with radiative recombination in the absorber (τ_2).

$$I_{PL}(t) = A_1 e^{\frac{-t}{\tau_1}} + A_2 e^{\frac{-t}{\tau_2}}, \quad (2)$$

where A_2 is a fitting constant. Since we standardized the measurement for all full devices and the only variable is the stoichiometric increase in sulfur in Zn(O,S), we focus the discussion on the PL decay profiles for full devices as a function of sulfur content in the buffer.

In all Zn(O,S) devices in their relaxed and light soaked states with the exception of the [O]:[S] = 1:1 device, τ_1 of < 10 ns was observed.[18] The short lifetime of τ_1 indicates efficient sweeping out of charges in the space charge region. Corresponding to the short lifetime and low intensity, the I-V curves for all sulfur-poor devices [Fig. 1(a)] and the light soaked 2:1 device [Fig. 1(b)] indicated good charge transport. τ_2 was only observed in the relaxed state of the 2:1 Zn(O,S) device and both states of the 1:1 device [Fig. 1(c)]. This was comparable to the profile of long decay lifetime for bare CIGS absorber from etched devices.[19] There is an increase in the TRPL intensity from [O]:[S] = 1:0–1:1 for both the relaxed and light soaked states, respectively. Under low injection, the PL intensity follows the product of the equilibrium hole concentration (p_0) and amount of excess electrons injected (Δn), $p_0 \Delta n$. When there is low defect density in the buffer, a stronger electric field leads to a more efficient charge separation of holes and electrons; hence, a short carrier lifetime and a small intensity are expected. Reduced strength of the electric field by a barrier in the p-n junction results in a much poorer separation and higher radiative recombination. As inferred from the TRPL data, devices in Table I mainly showed a small τ_1 and low PL peak intensity.

PL peak intensity were highest in the sulfur-rich [O]:[S] = 2:1 device at its relaxed state and [O]:[S] = 1:1 at both relaxed and light soaked states of 3.91×10^4–5.52×10^4 (a.u.), indicative of high radiative recombination. Light soaking the relaxed 2:1 device reduces the blocking of the current of the dark I-V profile [Fig. 1(b)]. On the corresponding TRPL decay curve, the τ_2 component disappears and the PL intensity is reduced [Fig. 1(d)]. Since the peak intensity reduces to 1.21×10^4 (a.u.), it can be inferred that excess acceptor states are compensated by light soaking that results in photo-doping of the buffer and improvement of charge separation and transportation in the device.[3,4] On the other hand, light soaking the 1:1 device did not significantly improve the device performance nor passivate its τ_2 component. It might be inferred that a high concentration of V_{Zn} or S_i acceptor states exists at this stoichiometry of sulfur in Zn(O,S) and it is not possible to improve the performance of the device by light soaking. The results here demonstrate a strong correlation of increasing metastability with increased sulfur content in the buffer. This causes an increasingly stronger blocking effect under forward bias the higher the sulfur content.

In order to validate the experimental observations, SCAPS-1D simulations representing the sulfur-poor, moderately sulfur-rich, and highly sulfur-rich cases were performed. Parameters representative of the real devices were first obtained from materials or electrical measurements. The absorber band gap was determined to be approximately 1.0 eV by external quantum efficiency measurements. Based on the XPS measurement of the absorber surface, the sulfur-rich, copper-poor absorber surface is expected to form an Ordered Vacancy Compound (OVC). For this reason, we added a 15 nm thick OVC to reflect type inversion (n-type) between the absorber and buffer.[20] The valence band maximum and conduction band minimum values of different ratios of Zn(O,S) synthesized were estimated using the XPS [S]/([S] + [O]) ratios, which were 0.10–0.22 for [O]:[S] = 1:0–1:1, depicted in Figure 2. As a result, except for pure ZnO where [O]:[S] = 1:0, any change in conduction band minimum was small and offset was assumed to be similar for sulfur-poor and sulfur-rich devices defined here.[21] Hence for all cases, CBO was set at +0.2 eV between the CIGSSe and Zn(O,S).

Resistivities of Zn(O,S) were found to be $5.79 \times 10^3\ \Omega/\square$ for the Zn(O,S) film of [O]:[S] = 4:1, $1.78 \times 10^9\ \Omega/\square$ for [O]:[S] = 2:1, and $1.84 \times 10^{10}\ \Omega/\square$ for [O]:[S] = 1:1. From AC Hall measurements, we were able to determine electron mobility ($8.58\ cm^2\ V^{-1}\ s^{-1}$) and carrier concentration

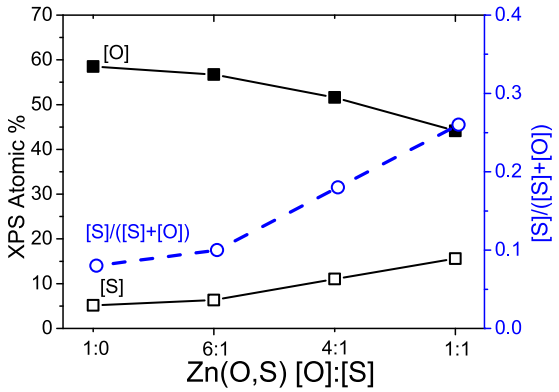

FIG. 2. Chemical compositions of Zn(O,S) films prepared on CIGSSe absorber as characterized by XPS with [O] (solid squares) and [S] (unfilled squares) and the calculated [S]/([S] + [O]) ratios.

$(1.65 \times 10^{19}\,\mathrm{cm}^{-3})$ for the [O]:[S] = 4:1 sample, comparable to values reported in literature.[22] In a compensated semiconductor material such as Zn(O,S), the net charge density ρ is the sum of holes (p) and electrons (n) as well as ionized acceptor (N_A) and donor atoms (N_D). It is expressed as $\rho = q(p - n + N_D - N_A)$, where q is the electric charge. Ionized acceptor states speculated to influence charge separation form a part of the total carrier concentration. As with other simulation studies,[23] the concentrations where ionized acceptor states influence distortion to the I-V curve are between 7.5×10^{17} and $1.3 \times 10^{18}\,\mathrm{cm}^{-3}$, and hence input parameters of acceptor density in the buffer in Table II were performed at this range. These acceptor states were defined at 1.0 eV above the valence band of the Zn(O,S),[8] with density

TABLE II. Input parameters for SCAPS-1D simulation of acceptor densities for sulfur-poor, moderately sulfur-rich, and highly sulfur-rich devices at relaxed and light soaked states where N_A is the density of (0/-) acceptors in the Zn(O,S) buffer.

State	Sulfur-poor Zn(O,S) N_A (cm^{-3})	Moderately sulfur-rich Zn(O,S) N_A (cm^{-3})	Highly sulfur-rich Zn(O,S) N_A (cm^{-3})
Relaxed	9.75×10^{17}	1.03×10^{18}	1.25×10^{18}
Light soaked	7.50×10^{17}	7.50×10^{17}	1.30×10^{18}

adjusted to simulate the relaxed and light soaked states for sulfur-poor and sulfur-rich Zn(O,S) devices. The capture cross section of holes for these acceptor states was assumed and set to $10^{-12}\,\mathrm{cm}^2$. The optical absorption parameter of the Zn(O,S) was estimated based on standard ZnO/ZnS absorption files.[24]

Figure 3 shows the I-V curves and electronic band structures of the CIGSSe solar cells constructed from SCAPS-1D simulation during their relaxed and light soaked states. Except for the highly sulfur-rich 1:1 device, we assume the light soaked states of the sulfur-poor and moderately sulfur-rich devices exhibit the same behavior and focused on comparing their relaxed states. For sulfur-poor Zn(O,S) devices, V_O and V_S donors predominate in the buffer and any addition of sulfur atoms fills up V_O and V_S until sulfur is in excess. When an excess of sulfur is introduced, as in the case of the moderately sulfur-rich Zn(O,S) device, V_{Zn} starts to predominate. An increase of V_{Zn} by 5% leads to a significant crossover for the relaxed device [cf. I-V curves in Figs. 3(a) vs. 3(b)]. At this state, excess acceptor states are occupied by electrons, and the

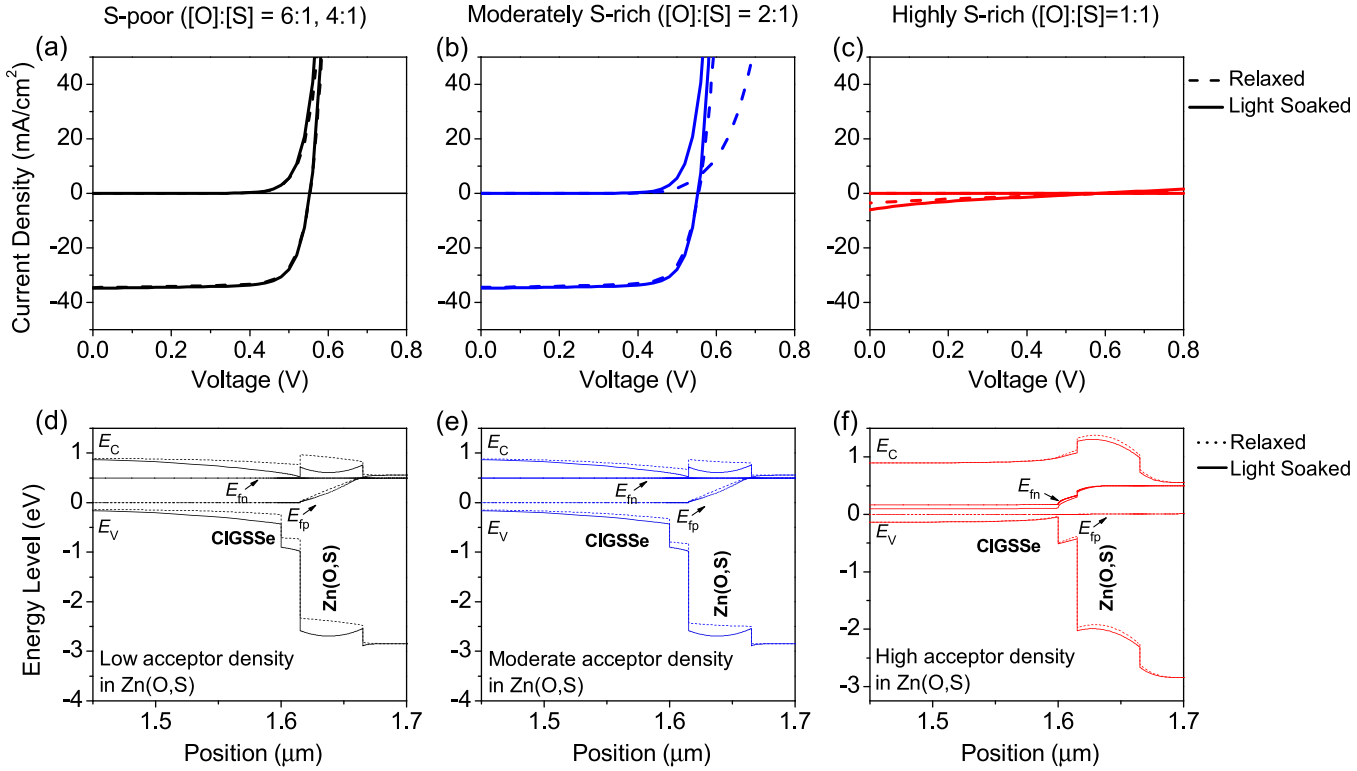

FIG. 3. Simulated I-V curves at relaxed (dashed lines) and light soaked states (solid lines) Zn(O,S) devices for (a) sulfur-poor Zn(O,S) devices and (b) moderately sulfur-rich Zn(O,S) devices and (c) highly sulfur-rich Zn(O,S) and the corresponding band diagrams at +0.5 V bias for (d) low sulfur content with low acceptor density, (e) moderately high sulfur content with moderate acceptor density, and (f) high sulfur content with high acceptor density.

conduction band and valence band of the Zn(O,S) are shifted upwards. This results in reduced band bending and reduced potential drop at the absorber/buffer interface at +0.5 V bias [cf. band diagrams in Figs. 3(d) vs. 3(e)]. Backflow of electrons to the absorber in Fig. 3(d) relaxed and hence recombination is enhanced, which agrees well with the high PL intensity observed in our experiment. The subsequent generation of electron-hole-pairs by light soaking leads to compensation of the negatively charged acceptor states in the buffer by holes, resulting in an optimal band alignment at the p-n junction with less potential drop across the buffer; hence, the electron quasi-fermi level (E_{fn}) at the interface gets closer to the conduction band minimum of Zn(O,S). For the highly sulfur-rich 1:1 device [Fig. 3(c)], the concentration of V_{Zn} acceptor states vastly exceeds the other cases. Under the same light soaking conditions, assuming the same extent of passivation of V_{Zn} acceptor states, this will result in a large barrier in the p-n junction whereby backflow of electrons is preferred [Fig. 3(f)]. Consequently, recombination is favored for both relaxed and light soaked states of this device and cell efficiency is close to 0%.

In this paper, we demonstrate that carrier lifetime τ_1 obtained with TRPL was in the range of <10 ns for sulfur-poor and moderately sulfur-rich Zn(O,S)/CIGSSe solar cells. For relaxed devices, there is increasing radiative recombination at the surface of the absorber with increasing sulfur content in the Zn(O,S) buffer. In addition, metastability in moderately sulfur-rich Zn(O,S) devices prone to relaxation and charge transport issues can be evaluated by the presence of a secondary, greater lifetime component τ_2 in relaxed solar cells. Light soaking generates photons to neutralize excess negative charges in the buffer of the moderately sulfur-rich Zn(O,S) device, reducing radiative recombination by improved charge separation and compensating the secondary lifetime component. On the other hand, highly sulfur-rich Zn(O,S) devices showed no improvement in the I-V characteristics before and after light soaking, indicating radiative recombination is still dominant and charge separation in the device is poor. The results here demonstrate good correlation of the increasing sulfur content to the appearance of the secondary lifetime component, implying an increased density of acceptor states leads to worsening I-V characteristics. This leads to a better understanding of metastability and charge transport issues in the Zn(O,S) buffered devices. When selecting the stoichiometry of the buffer for fabrication of devices, one might consider a relatively sulfur-poor Zn(O,S) of 4:1 ratio device that achieves sufficiently high J_{SC} and V_{OC} and avoid metastability at the same time. This would ensure a stable solar cell output that does not fluctuate due to dark storage. On the extreme ends, a 0:1 ratio (pure ZnO) will lead to low V_{OC} due to band alignment mismatch with the CIGSSe absorber. A sulfur-rich 1:1 ratio favors the formation of excessive acceptor states in the buffer, distorting the I-V curve and resulting in a low J_{SC} and FF. With these considerations, the optimal stoichiometry of [O]:[S] in the buffer should be 4:1 ratio to obtain a device of high efficiency and low metastability.

We would like to thank the Bosch Solar CISTech GmbH for the CIGSSe absorbers and for TRPL measurements. We would also like to thank Ms. Tetiana Lavrenko for additional I-V measurements. R. H. Chua acknowledges the funding support from the Economic Development Board of Singapore (EDB), through the Industrial Postgraduate Program (IPP).

[1]D. Hariskos, S. Spiering, and M. Powalla, Thin Solid Films **480–481**, 99 (2005).
[2]I. L. Eisgruber, J. E. Granata, J. R. Sites, J. Hou, and J. Kessler, Sol. Energy Mater. Sol. Cells **53**(3–4), 367 (1998).
[3]A. O. Pudov, J. R. Sites, M. A. Contreras, T. Nakada, and H. W. Schock, Thin Solid Films **480–481**, 273 (2005).
[4]M. Igalson, A. Urbaniak, P. Zabierowski, H. A. Maksoud, M. Buffiere, N. Barreau, and S. Spiering, Thin Solid Films **535**, 302 (2013).
[5]K. Kushiya, S. Kuriyagawa, K. Tazawa, T. Okazawa, and M. Tsunoda, paper presented at the Conference Record of the 2006 IEEE 4th World Conference on Photovoltaic Energy Conversion, 2006; Y. Okuda, paper presented at the 2012 IEEE International Reliability Physics Symposium, 2012; W. Witte, D. Hariskos, and M. Powalla, Thin Solid Films **519**(21), 7549 (2011).
[6]C. Platzer-Björkman, T. Törndahl, A. Hultqvist, J. Kessler, and M. Edoff, Thin Solid Films **515**(15), 6024 (2007).
[7]T. Song, J. T. McGoffin, and J. R. Sites, IEEE J. Photovoltaics **4**(3), 942 (2014).
[8]J. B. Varley and V. Lordi, Appl. Phys. Lett. **103**(10), 102103 (2013).
[9]A. Niemegeers and M. Burgelman, J. Appl. Phys. **81**(6), 2881 (1997).
[10]V. Probst, I. Koetschau, E. Novak, A. Jasenek, H. Eschrich, F. Hergert, T. Hahn, J. Feichtinger, M. Maier, B. Walther, and V. Nadenau, IEEE J. Photovoltaics **4**(2), 687 (2014).
[11]A. Shimizu, S. Chaisitsak, T. Sugiyama, A. Yamada, and M. Konagai, Thin Solid Films **361–362**, 193 (2000); E. B. Yousfi, B. Weinberger, F. Donsanti, P. Cowache, and D. Lincot, *ibid.* **387**(1–2), 29 (2001); T. Kobayashi, T. Kumazawa, L. Kao, and T. Nakada, Sol. Energy Mater. Sol. Cells **119**, 129 (2013); E. B. Yousfi, T. Asikainen, V. Pietu, P. Cowache, M. Powalla, and D. Lincot, Thin Solid Films **361–362**, 183 (2000); J. R. Bakke, J. T. Tanskanen, C. Hägglund, T. A. Pakkanen, and S. F. Bent, J. Vac. Sci. Technol. A **30**(1), 01A135 (2012).
[12]J. A. Woollam, see http://www.jawoollam.com/pdf/Alpha_Brochure.pdf for details on measuring thin films on glass by the Alpha-SE system.
[13]D. V. O'Connor and D. Phillips, *Time-Correlated Single Photon Counting* (Academic Press, London, Orlando, 1984).
[14]M. P. Seah, I. S. Gilmore, and S. J. Spencer, Surf. Sci. **461**(1–3), 1 (2000).
[15]J. H. Scofield, J. Electron. Spectrosc. Relat. Phenom. **8**(2), 129 (1976).
[16]O. Gunawan and T. Gokmen, U.S. patent 9,041,389 (2015); O. Gunawan, Y. Virgus, and K. F. Tai, Appl. Phys. Lett. **106**, 062407 (2015); Dev. Team: O. Gunawan, T. Gokmen, K. F. Tai, Y. Virgus, and M. Pereira, IBM Research, 2015.
[17]R. K. Ahrenkiel, Solid-State Electron. **35**(3), 239 (1992).
[18]M. Maiberg and R. Scheer, J. Appl. Phys. **116**(12), 123710 (2014); M. Maiberg and R. Scheer, *ibid.* **116**(12), 123711 (2014).
[19]W. K. Metzger, I. L. Repins, and M. A. Contreras, Appl. Phys. Lett. **93**(2), 022110 (2008); W. K. Metzger, I. L. Repins, M. Romero, P. Dippo, M. Contreras, R. Noufi, and D. Levi, Thin Solid Films **517**(7), 2360 (2009).
[20]D. Schmid, M. Ruckh, F. Grunwald, and H. W. Schock, J. Appl. Phys. **73**(6), 2902 (1993).
[21]B. K. Meyer, A. Polity, B. Farangis, Y. He, D. Hasselkamp, Th. Krämer, and C. Wang, Appl. Phys. Lett. **85**(21), 4929 (2004); T. Adler, Ph.D. thesis, Technische Universität Darmstadt, 2013.
[22]H. H. Park, R. Heasley, and R. G. Gordon, Appl. Phys. Lett. **102**(13), 132110 (2013); H. H. Park, A. Jayaraman, R. Heasley, C. Yang, L. Hartle, R. Mankad, R. Haight, D. B. Mitzi, O. Gunawan, and R. G. Gordon, *ibid.* **105**(20), 202101 (2014).
[23]N. Naghavi, S. Temgoua, T. Hildebrandt, J. F. Guillemoles, and D. Lincot, Prog. Photovoltaics **23**, 1820–1827 (2015).
[24]S. Adachi, *Optical Constants of Crystalline and Amorphous Semiconductors: Numerical Data and Graphical Information* (Springer US, 2013).